

Towards a safe non-invasive method for evaluating the carbonate substitution levels of hydroxyapatite (HAP) in micro-calcifications found in breast tissue†

Marleen M. Kerssens,^{ab} Pavel Matousek,^c Keith Rogers^b and Nicholas Stone^{*a}

Received 23rd July 2010, Accepted 22nd September 2010

DOI: 10.1039/c0an00565g

A new diagnostic concept based on deep Raman spectroscopy is proposed permitting the non-invasive determination of the level of carbonate substitution in type II calcifications (HAP). The carbonate substitution has shown to be directly associated with the pathology of the surrounding breast tissue and different pathology groups can therefore be separated using specific features in the Raman spectra of the calcifications. This study explores the principle of distinguishing between type II calcifications, found in proliferating lesions, by using the strongest Raman peak from calcium hydroxyapatites (the phosphate peak at 960 cm⁻¹) to act as a surrogate marker for carbonate substitution levels. It is believed that carbonate ion substitution leads to a perturbation of the hydroxyapatite lattice which in turn affects the phosphate vibrational modes. By studying calcifications, with known carbonate content, buried in porcine tissue it has been possible to evaluate the feasibility of using the proposed approach to probe the composition of the calcifications *in vivo* and hence provide pathology specific information non-invasively, in real time. Using the proposed concept we were able to determine the level of carbonate substitutions through soft tissue phantom samples (total thickness of 5.6 mm). As the level of carbonate substitution has been previously correlated with mid-FTIR to the lesion type, *i.e.* whether benign or invasive or *in situ* carcinoma, the new findings provide a major step forward towards establishing a new capability for diagnosing benign and malignant lesions in breast tissue in a safe and non-invasive manner *in vivo*.

Introduction

The accurate and safe diagnosis of breast cancer is a significant issue, with annual incidence of 44 000 women and around 300 men in the UK. Early diagnosis of the disease allows more conservative treatments and better patient outcomes.¹

Microcalcifications in the breast are an important indicator for cancer, and often the only sign of its presence. Several studies have suggested that the type of calcification formed may act as a marker for malignancy, that its presence may be of biological significance, and that the chemical composition can indicate disease state.^{2–5}

In the breast, two types of microcalcifications are commonly found. Type I consists of calcium oxalate dihydrate (COD) and is mostly associated with benign lesions.^{2,6} Type II consists of calcium phosphate, mostly hydroxyapatite (HAP), and is associated with both benign and malignant pathologies.^{2,3}

Although mammography can, to some extent, detect the presence of calcifications in tissue, it is unable to yield any information on their chemical composition and thus cannot provide a definitive marker for classifying benign and malignant

lesions. This is currently a significant health issue as only 10–25% of mammographically detected lesions are found to be malignant^{7,8} by subsequent needle biopsy.

Our earlier studies have established that the distinctly different types I and II can be detected and separated non-invasively using transmission Raman spectroscopy through up to 27 mm of soft tissue^{9–11} (Fig. 1) providing a basic building block for a non-invasive diagnostic tool based around Raman spectroscopy. As stated above the detection of type I calcifications in such a method would signal the presence of benign lesion. However, if type II calcifications were identified the diagnosis would be ambiguous as both benign or malignant lesion could be present. A study of Haka *et al.*³ has shown that there are significant differences in the level of carbonate substitution in type II calcifications and these can be related to the pathology too; benign proliferative lesions have type II calcifications with higher carbonate levels than those of the HAP found in malignant lesions. Recent work of Baker *et al.*¹² showed that pathology groups could be separated even further to include both invasive and *in situ* breast lesions. This is based on the amide : phosphate ratio and the percentage of carbonate substitution measured with FTIR spectroscopy (Fourier Transform (mid-)Infrared). However, FTIR cannot easily be used *in vivo* because IR light is strongly absorbed by water. Since Raman spectroscopy has been shown to have a considerable potential for being used non-invasively *in vivo*,^{10,11,13–17} accurate analysis of the carbonate levels in type II calcifications with Raman spectroscopy would enable the removal of any ambiguity at mammography in separating the benign and malignant lesions with type II calcifications. By doing this non-invasively through the breast this would eliminate the need for biopsies and thus reduce patient trauma, costs and time delays.

^aBiophotonics Research Unit, Gloucestershire Royal Hospital, Great Western Road, Gloucester, Gloucestershire, GL1 3NN, UK. E-mail: n.stone@medical-research-centre.com

^bCranfield Health, Cranfield University, Cranfield, Bedfordshire, MK43 0AL, UK

^cCentral Laser Facility, Research Complex at Harwell, Science and Technology Facilities Council, Rutherford Appleton Laboratory, Didcot, Oxfordshire, OX11 0QX, UK

† This article is part of a themed issue on Optical Diagnosis. This issue includes work presented at SPEC 2010 Shedding Light on Disease: Optical Diagnosis for the New Millennium, which was held in Manchester, UK June 26th–July 1st 2010.

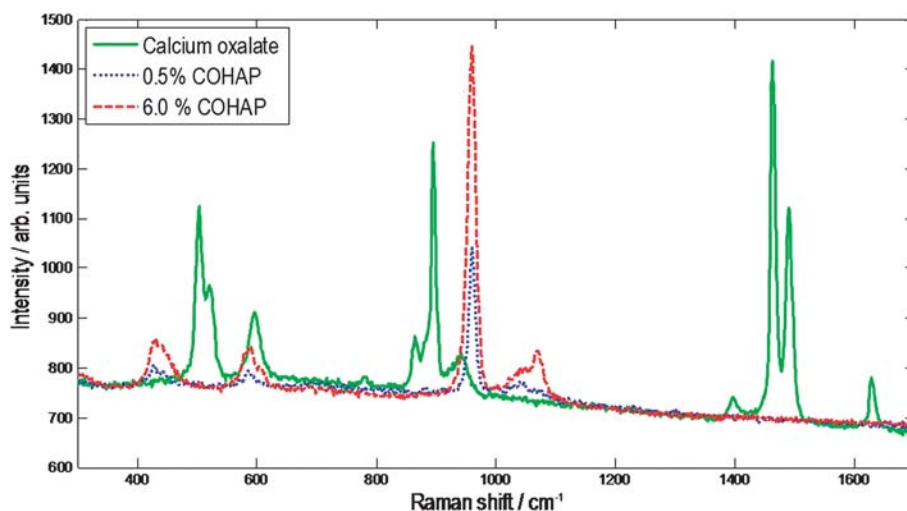


Fig. 1 Raman spectrum of calcium oxalate (type I) and 0.5 and 6.0% carbonate substituted hydroxyapatite (COHAP, type II calcification). As can be seen the carbonate features of the COHAP samples are relatively weak (~ 1042 and ~ 1070 cm^{-1}) compared with the intensity of the phosphate peak (~ 960 cm^{-1}).

Normally, the relative intensities of the intense phosphate band at ~ 960 cm^{-1} and a much weaker carbonate band at ~ 1070 cm^{-1} in Raman experiments are used to quantify the relative amount of carbonate substitution (see Fig. 1). Unfortunately, the carbonate peak has a relatively low intensity and therefore could be hard to measure *in vivo*. This is in contrast with the band at ~ 960 cm^{-1} that has a very high relative intensity. Previous work has demonstrated that the width (full width half maximum—FWHM) of many vibrational bands increases in carbonated phases with the level of carbonate content and therefore the FWHM of the most intense peak at 960 cm^{-1} could be a better quantitative marker for the level of carbonate substitution in deep subsurface studies.^{18–20} A higher FWHM indicates a reduction in crystallinity (*i.e.* an increase in disorder) caused by higher carbonate content. Furthermore, small peak shifts of the same band also indicated in literature^{21,22} appear related to the degree of crystallinity and hence carbonate ion substitution.

The aim of this study is to assess the feasibility of evaluating the amount of carbonate substitution based on properties of the most intense peak at ~ 960 cm^{-1} (width and position) through a layer of tissue, an issue of high clinical relevance.

Materials and methods

Samples

There are three different types of substitution mechanisms possible for the incorporation of carbonate within the lattice for type II calcifications. In A-type substitutions CO_3^{2-} replaces the OH^- lattice ions, in B-type substitutions the CO_3^{2-} takes the position of the PO_4^{3-} , and in L-type (labile) the CO_3^{2-} is within the surface hydration layer of the apatite crystals. Since the carbonate has a charge different from the ions it replaces, the charge has to be compensated by other exchanges, for example Ca^{2+} by Na^+ . It is thought that most, if not all, carbonate substitutions in breast calcifications are B-type.²³ Therefore we have obtained B-type carbonate apatite from Clarkson Chromatography (South Williamsport, PA, USA) to use as standards.

The standards had a carbonate substitution percentage of 0.5, 1.4, 2.0, 2.3, and 3.5, 6.0, and 11.0%, as defined by the manufacturer ($\pm 1\%$) using FTIR and validated by us using X-ray diffraction. The powders were used without further sample pretreatment and placed in quartz cuvettes with a path length of 2 mm (Starna) for the experiments described.

Experimental setup

A scheme of the experimental setup is shown in Fig. 2. The emission from a frequency stabilized laser module (830 nm,

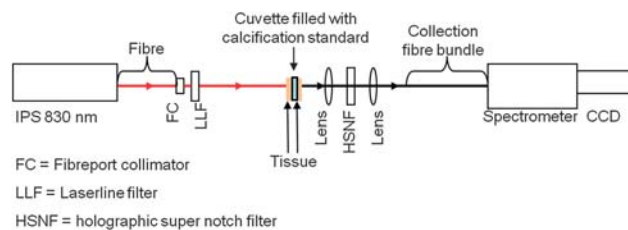


Fig. 2 Illustration of the used setup.

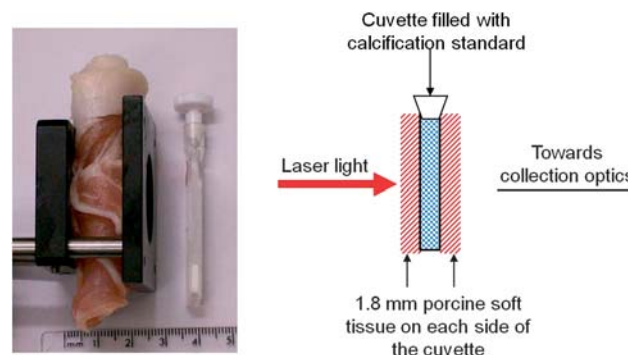


Fig. 3 Details of the experimental setup. Left panel: porcine tissue wrapped around an optical cell was used in the non-invasive experiments. Right panel: schematic representation.

Innovative Photonics Solutions) is sent from a fibre (Ceram-Optec, 'spot to slit line' type bundle assembly, active area spot approximately 2.21 mm, slit line approximately 0.25 mm × 14.95 mm) to a fibre export collimator (Thorlabs) and passed through a laser line filter (FL830-10, Thorlabs) to suppress off-centre spectral emission from the laser line. The sample was illuminated with 130 mW of light in a 4 mm spot. The generated Raman signal was collected in transmission mode using an AR coated lens ($f = 60$ mm, dia. = 50 mm, INGCYRS Laser systems). The collimated scattered light was passed through a holographic

super notch filter (HSPF-830.0 AR-2.0, Kaiser Optical Systems) to remove the elastically scattered light and imaged onto a fibre probe bundle by a second lens of the identical parameters to the collection lens. The output end of the fibre probe was placed at the entrance port of a Holospec VPH system spectrograph (Kaiser Optical systems Inc, HSG-917.4 custom). Spectra of the standards were collected with an accumulation time of 20 seconds using a CCD camera cooled to -70 °C (Andor Technology, DU420A-BR-DD, 1024 × 255 pixels). The samples were each measured five times in random order. In a non-invasive

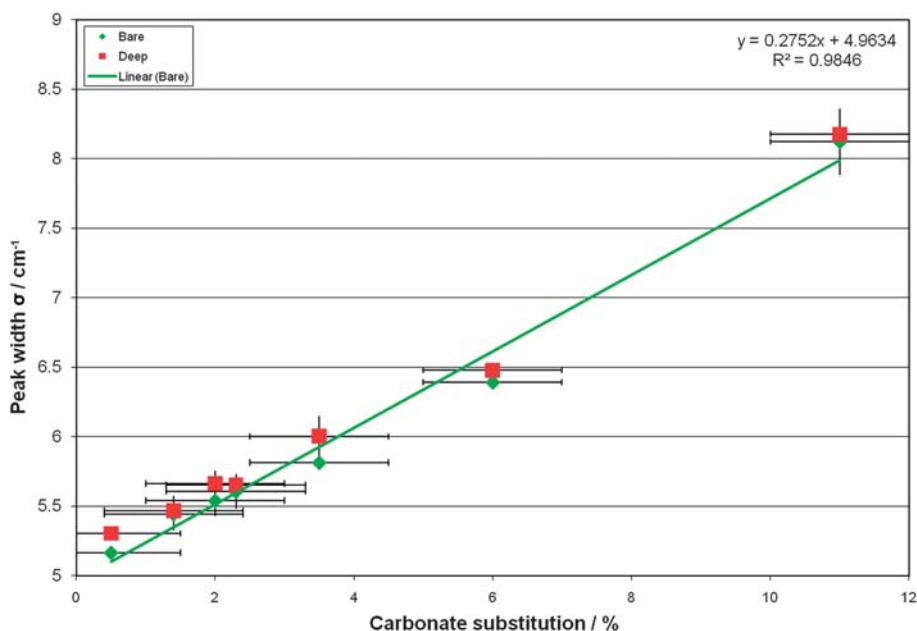


Fig. 4 Peak width *versus* carbonate substitution; the bare calcification standards are plotted as green diamonds (mean values) and a linear function was fit to provide a calibration function for the standards buried in 3.6 mm of porcine tissue (mean values shown in red squares). Error bars show the uncertainty in the carbonate substitution values provided by the manufacturer and the standard deviation of the replicate values of the spectral peak width.

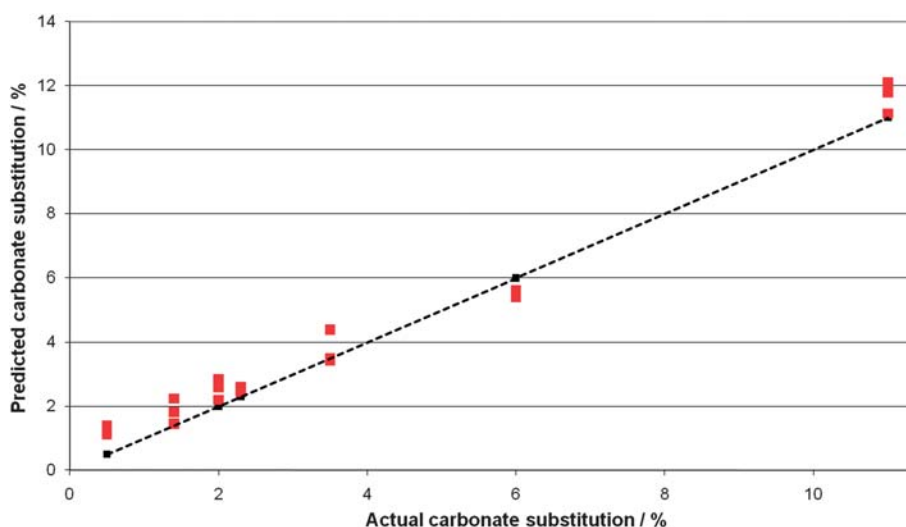


Fig. 5 Predicted *versus* actual carbonate substitution of the buried material based on the width of the 960 cm^{-1} phosphate peak.

Table 1 Prediction of the percentage carbonate substitution based on the width of the peak

Carbonate substitution according to supplier (quoted as $\pm 1\%$)	Mean predicted carbonate percentage through tissue (± 1 std)	Root mean square error of prediction (% carbonate)
0.5%	1.22 ± 0.14	0.75
1.4%	1.83 ± 0.39	0.54
2.0%	2.55 ± 0.33	0.61
2.3%	2.51 ± 0.07	0.22
3.5%	3.78 ± 0.53	0.52
6.0%	5.51 ± 0.17	0.50
11.0%	11.68 ± 0.50	0.79

proof-of-principle feasibility study the cuvettes were wrapped in porcine tissue (shown in Fig. 3) to evaluate the carbonate substitution through a layer of tissue. Tissue with a mix of fat and protein was chosen to mimic bulk human breast tissue. The thickness of the porcine tissue was 1.8 mm for the proof of principle experiments on both sides of the cuvettes (overall thickness of porcine tissue $3.6 \text{ mm} + 2 \text{ mm cuvette} = 5.6 \text{ mm}$). In this study the signal was accumulated over 5×60 seconds and the cosmic ray removal option of the detector software was used. The system was calibrated using Raman bands of an aspirin tablet (acetylsalicylic acid) and had a spectral resolution of 5.8 cm^{-1} .

Data analysis

All data were loaded into Matlab7 (The Mathworks) in which an in-house written tool fitted a Gaussian to the band located at 960 cm^{-1} and its bandwidth σ (where the $\text{FWHM} \approx 2.35\sigma$) and position were evaluated.

Results and discussion

The mean peak width (σ) for each of the bare standard samples (five replicate measurements) was plotted against the calcification substitution percentage. A linear function was fit to these points, shown in Fig. 4, and the mean values for the buried calcifications were also plotted (three replicates). It can be seen that the buried calcification standards have peak widths within a standard deviation of each other (shown with error bars). The equation of the line calculated from the spectra of bare standards was used to provide a prediction of the carbonate substitution percentage of the buried standards. Fig. 5 shows the results plotted against actual concentration determined by the manufacturer with FTIR. Table 1 shows the root-mean-square-error of these predictions.

The mean peak position for each of the bare standard samples (five replicate measurements) was plotted against the calcification substitution percentage. A logarithmic function was fit to these points, shown in Fig. 6, and the mean values for the buried calcifications were also plotted (three replicates). It can be seen that the buried calcification standards have peak positions within a standard deviation of each other (shown with error bars). The logarithmic function was used to provide a prediction of the carbonate substitution percentage of the buried standards. Fig. 7 shows the results plotted against actual concentration. Table 2 shows the root-mean-square-error of these predictions.

As can be seen in Fig. 4 and 6, the width of the peak increases with a higher carbonate substitution, while the position of the phosphate peak moves to lower Raman wavenumber with higher carbonate substitution. There is some subtle variability in the width and position of the phosphate peak between measurements from different areas of the same sample. It is thought to be due to the heterogeneous nature of the apatite standards used. Also, a systematic difference in width between bare and buried samples

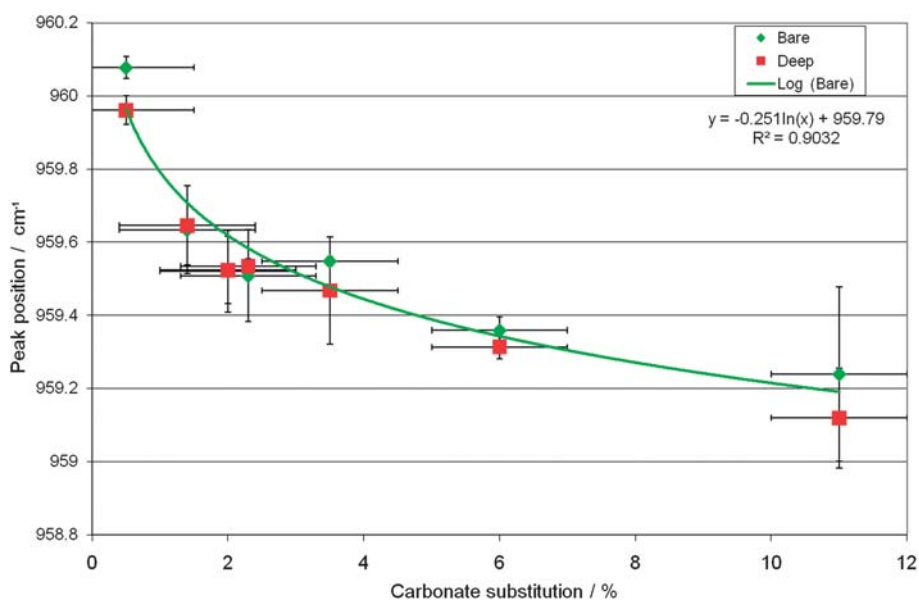


Fig. 6 Peak position *versus* carbonate substitution; the bare calcification standards are plotted as green diamonds (mean values) and a logarithmic function was fit to provide a calibration function for the standards buried in 3.6 mm of porcine tissue, total thickness 5.6 mm (mean values shown in red squares). Error bars show the uncertainty in the carbonate substitution values provided by the manufacturer and the standard deviation of the replicate values of the spectral peak position.

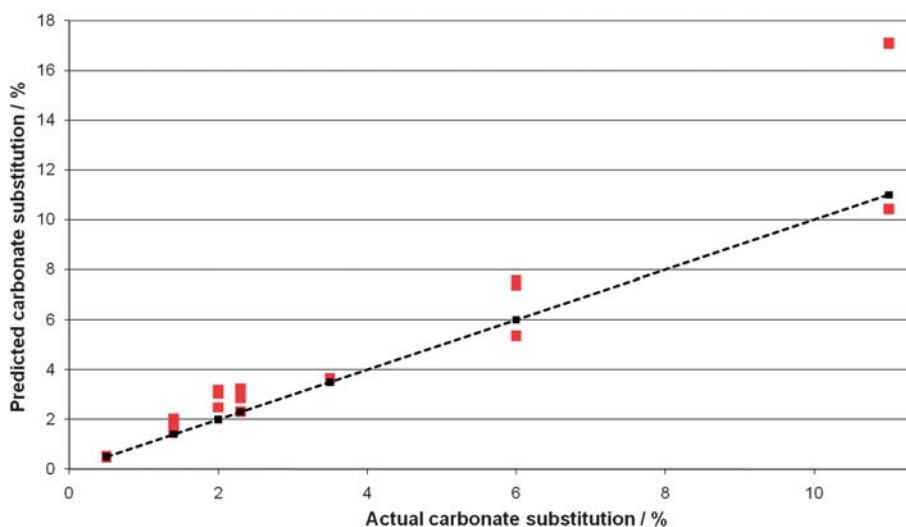


Fig. 7 Predicted versus actual carbonate substitution of the buried material based on the position of the 960 cm^{-1} phosphate peak.

Table 2 Prediction of the carbonate substitution based on the peak position

Carbonate substitution according to supplier (quoted as $\pm 1\%$)	Mean predicted carbonate percentage through tissue (± 1 std)	Root mean square error of prediction (% carbonate)
0.5%	0.51 ± 0.04	0.03
1.4%	1.79 ± 0.23	0.43
2.0%	2.91 ± 0.37	0.96
2.3%	2.80 ± 0.46	0.63
3.5%	3.61 ± 0.05	0.12
6.0%	6.77 ± 1.23	1.26
11.0%	14.88 ± 3.85	4.99

can be observed which is believed to be caused by the S/N ratio of the buried samples. When signal was acquired for a longer period of time these differences were not observed. The region of interest (clinically relevant area) is between 0.5% and 2.5% and is based on work of Baker *et al.*¹² which indicated that calcifications corresponding to benign pathology have an average carbonate substitution around 2%. This percentage is lower for calcifications corresponding to *in situ* and invasive pathology; where the amount of carbonate substitution is $\sim 1.7\%$ and $\sim 1.4\%$ on average, respectively. The data of these three pathology groups show a spread from 0.5 to 2.5% carbonate substitution.

The relationship between the carbonate substitution and the width in the relevant area seems to be approximately linear. In contrast, the relationship between the carbonate substitution and the position in the clinically relevant area shows a semi-exponential trend. In agreement to the work presented here, it has been reported previously that the width of the 960 cm^{-1} band is linearly correlated to the carbonate concentration in breast calcifications.³ It should be noted that the carbonate substitution can be most accurately predicted using the peak width, although in samples with relatively low carbonate content between 0.5 and 3.5% (the clinically important range for this proposed

application) the peak position has a slightly lower sum of root-mean-squared prediction errors. This is reversed for buried standards with greater than 3.5% carbonate substitution.

In order to use the level of carbonate substitution as a clinical diagnostic tool, more knowledge must be obtained concerning the different types of carbonate substitution in type II breast calcifications and the relationship between this and the width and position of the Raman band at $\sim 960\text{ cm}^{-1}$, as well as other potential sources of broadening. It must be noted that we are not directly measuring the carbonate within the breast calcification standards and are therefore making the assumption that the change in features of the 960 cm^{-1} peak is attributable to the carbonate. This is not unreasonable, and certainly correlates well, however, there are other structural changes that may occur that could also modify the peak—in fact any disordering mechanism could do this.

Conclusions

Samples with different amounts of carbonate substitution can be separated both with the position and the width of the Raman peak located at 960 cm^{-1} . It has also been shown that indication of the carbonate substitution based on the peak located at 960 cm^{-1} is feasible when measured through biological tissue, where porcine tissue was used as a human breast tissue phantom in this study. As part of this feasibility study we also explored the limits under which this method could be used with the described experimental configuration. Peak characteristics were also measured from spectra measured from an overall tissue depth of 16 mm of porcine soft tissue (not shown), with minimal data analysis. Further analysis with chemometric tools such as PCA would be likely to enable greater signal recovery.

This study paves the way towards a new generation of non-invasive breast screening methods based around transmission Raman and spatially offset Raman spectroscopy (SORS). Since the proposed method of pathological discrimination is based upon measuring only the strongest calcification peak, signals

from deeper in the tissue can be used or measurements can be performed in shorter timescales than if the analysis required a conventional calculation of the direct intensity ratio of the weak carbonate and strong phosphate Raman bands.

Acknowledgements

We would like to thank Gavin R. Lloyd for his help with the Matlab fitting routine. Nick Stone holds a Senior (Career Scientist) Research Fellowship funded by the UK National Institute of Health Research. Marleen Kerssens holds a doctoral research fellowship jointly funded by Gloucestershire Hospitals NHS Foundation Trust and the Science and Technology Facilities Council's Biomedical Network (4161234).

References

- 1 NHS, *NHS Breast Screening Programme Annual Review 2008*, 2008.
- 2 M. J. Radi, *Arch. Pathol. Lab. Med.*, 1989, **113**, 1367–1369.
- 3 A. S. Haka, K. E. Shafer-Peltier, M. Fitzmaurice, J. Crowe, R. R. Dasari and M. S. Feld, *Cancer Res.*, 2002, **62**, 5375–5380.
- 4 M. P. Morgan, M. M. Cooke and G. M. McCarthy, *J. Mammary Gland Biol. Neoplasia*, 2005, **10**, 181–187.
- 5 M. P. Morgan, M. M. Cooke, P. A. Christopherson, P. R. Westfall and G. M. McCarthy, *Mol. Carcinog.*, 2001, **32**, 111–117.
- 6 N. Singh and J. M. Theaker, *J. Clin. Pathol.*, 1999, **52**, 145–146.
- 7 A. S. Haka, K. E. Shafer-Peltier, M. Fitzmaurice, J. Crowe, R. R. Dasari and M. S. Feld, *Proc. Natl. Acad. Sci. U. S. A.*, 2005, **102**, 12371–12376.
- 8 A. J. Evans, A. R. M. Wilson, H. C. Burrell, I. O. Ellis and S. E. Pinder, *Clin. Radiol.*, 1999, **54**, 644–646.
- 9 P. Matousek and N. Stone, *Analyst*, 2009, **134**, 1058–1066.
- 10 N. Stone and P. Matousek, *Cancer Res.*, 2008, **68**, 4424–4430.
- 11 P. Matousek and N. Stone, *J. Biomed. Opt.*, 2007, **12**, 024008.
- 12 R. N. Baker, K. D. Rogers, N. Shepherd and N. Stone, *Br. J. Cancer*, 2010, **103**, 1034–1039.
- 13 P. Matousek, I. P. Clark, E. R. C. Draper, M. D. Morris, A. E. Goodship, N. Everall, M. Towrie, W. F. Finney and A. W. Parker, *Appl. Spectrosc.*, 2005, **59**, 393–400.
- 14 M. V. Schulmerich, K. A. Dooley, M. D. Morris, T. M. Vanasse and S. A. Goldstein, *J. Biomed. Opt.*, 2006, **11**, 060502.
- 15 M. V. Schulmerich, J. H. Cole, K. A. Dooley, M. D. Morris, J. M. Kreider, S. A. Goldstein, S. Srinivasan and B. W. Pogue, *J. Biomed. Opt.*, 2008, **13**, 020506.
- 16 N. A. Macleod and P. Matousek, *Appl. Spectrosc.*, 2008, **62**, 291A–304A.
- 17 N. Stone, R. Baker, K. Rogers, A. W. Parker and P. Matousek, *Analyst*, 2007, **132**, 899–905.
- 18 A. Awonusi, M. D. Morris and M. M. J. Tecklenburg, *Calcif. Tissue Int.*, 2007, **81**, 46–52.
- 19 A. Krajewski, M. Mazzocchi, P. L. Buldini, A. Ravaglioli, A. Tinti, P. Taddei and C. Fagnano, *J. Mol. Struct.*, 2005, **744–747**, 221–228.
- 20 F. F. M. de Mul, M. H. J. Hottenhuis, P. Bouter, J. Greve, J. Arends and J. J. ten Bosch, *J. Dent. Res.*, 1986, **65**, 437–440.
- 21 G. Penel, G. Leroy, C. Rey and E. Bres, *Calcif. Tissue Int.*, 1998, **63**, 475–481.
- 22 J. D. Pasteris, B. Wopenka, J. J. Freeman, K. Rogers, E. Valsami-Jones, J. A. M. van der Houwen and M. J. Silva, *Biomaterials*, 2004, **25**, 229–238.
- 23 K. D. Rogers and R. A. Lewis, in *Breast Calcification: a Diagnostic Manual*, ed. A. Evans, S. Pinder, R. Wilson and I. Ellis, Greenwich Medical Media, 2002, pp. 171–189.